# Optimization of the scintillator units for the CEPC scintillator-tungsten ECAL

Bing Zhao[1,5] · Mingyi Dong[1,2,3] · Ming Zhou[1] · Zhigang Wang[1,2] · Hang Zhao[1,2] · Yazhou Niu[4] · Tao Hu[1,2,3] · Shujun Zhao[5]

## Abstract

**Background** The circular electron positron collider (CEPC) was proposed as a future Higgs/Z factory. A sampling calorimeter with scintillator-tungsten sandwich structure (ScW) is selected as one of the electromagnetic calorimeter (ECAL) options. Its active layers consist of plastic scintillator strip units with a thickness of 2 mm and a size of $5 \times 45$ mm$^2$, read out by silicon photomultipliers (SiPM).

**Purpose** The light output has non-uniformity along the length direction of the scintillator strip, which affects the resolution of the ScW ECAL. It is necessary to control the non-uniformity to a low level.

**Methods** We present the optimization of the scintillator units to improve the uniformity of the light output, including the light output distribution of the scintillator strips with different SiPM coupling configurations, and the impact of the coupling groove shape and dimension on the light output uniformity.

**Results and conclusion** The results show that the non-uniformity of the scintillator unit with a runway-shaped coupling groove at the bottom-center of the strip can achieve 4% without reduction in the light output. Compared to the case of non-uniformity before optimization, the optimized uniformity improves the boson mass resolution about 23% based on the reconstruction of Higgs $\rightarrow \gamma\gamma$, which is comparable to the perfect homogeneous case.

**Keywords** CEPC · ECAL · SiPM · Uniformity · Scintillator

## Introduction

The circular electron positron collider (CEPC) [1] is a large international scientific facility proposed by the Chinese particle physics community in 2012. It is designed with a circumference of about 100 km to be as a Higgs and Z factory. A particle flow algorithm (PFA) [2] oriented calorimetry

system is adopted as current baseline design in the CEPC detectors to provide hermetic coverage for high-resolution energy measurements of electrons, photons, taus and hadronic jets. A sampling electromagnetic calorimeter (ECAL) with scintillator-tungsten sandwich structure (ScW), derived from the CALICE scintillator ECAL developments [3, 4], is selected as one of the CEPC ECAL options. It can be built in a compact and cost-effective way. Major design parameters of the ScW ECAL were studied and optimized by Monte Carlo (MC) simulation. The ScW ECAL is composed of about 30 layers in the longitudinal direction. Each layer includes a 2.8-mm-thick tungsten plate absorber, a 2-mm-thick scintillator active layer and an embedded readout printed circuit board (PCB). Each active layer consists of scintillator strip units with a thickness of 2 mm and a size of $5 \times 45$ mm$^2$ [5, 6]. The number of readout channels can be significantly reduced due to the strip structure. The scintillator strips in adjacent layers are arranged perpendicularly to each other to achieve a small effective transverse readout cell size of about $5 \times 5$ mm$^2$. Each strip is covered by a

✉ Mingyi Dong
dongmy@ihep.ac.cn

1  Institute of High Energy Physics, Chinese Academy of Sciences, Beijing 100049, China

2  State Key Laboratory of Particle Detection and Electronics, Beijing 100049, China

3  University of Chinese Academy of Sciences, Beijing 100049, China

4  University of Science and Technology of China, Hefei 230026, China

5  Zhengzhou University, Zhengzhou 450001, China

reflector film to increase the light collection efficiency and prevent the optical cross talk between the scintillator strips. Photons from each scintillator strip are read out by a silicon photomultiplier (SiPM) attached to the strip. The SiPM and highly integrated readout electronics make the dead area in the scintillator-tungsten ECAL almost negligible.

The light output has non-uniformity along the length of the scintillator, which has an impact on the performance of the ScW ECAL. To achieve a good uniformity along the whole scintillator strip, the optimization of the scintillator unit, including the coupling configuration of the SiPM to the scintillator strip, is needed. In this paper, the experimental study and optimization of the scintillator unit design are presented.

## Setup of the test system and calibration

The minimum ionized particle (MIP) signal is usually used for the scintillator units test. The electrons generated by the decay of a $^{90}Sr$ are used to simulate the MIPs in the test. The scintillator strip under test wrapped with an enhanced specular reflector (ESR) film is attached to a PCB and read out by a Hamamatsu S12571-010P SiPM. The S12571-010P SiPM with 1 mm × 1 mm active area and 10 μm pitch size is selected based on the dynamic range requirement of the ScW ECAL. The PCB is fixed on an automatic motor and can be moved along the length direction of the scintillator strip. The electrons pass through the scintillator unit along the Z direction. A plastic scintillation fiber (BCF-10) with a diameter of 1 mm read out by another SiPM is placed below the scintillator unit to provide trigger signals, as shown in Fig. 1. The relative position of the trigger fiber and the $^{90}Sr$ source are fixed. By moving the scintillator strip, the light output is tested with the incident electrons passing though different positions of the strip to characterize the uniformity of the light output.
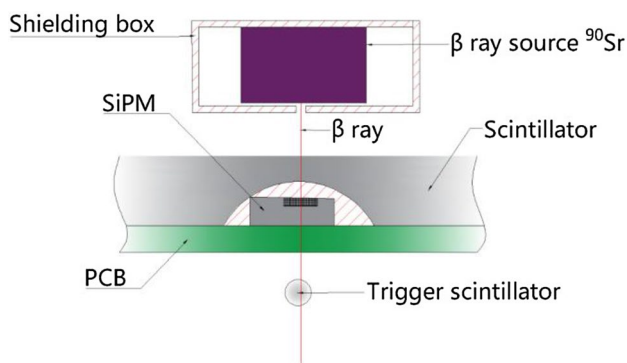
The SiPM from the scintillator unit is connected to a Hamamatsu driver board (C12332-01), which not only amplifies the signals, but also has a temperature compensation circuit to keep a stable gain during the test. The signals from the driver board together with the trigger signals are sent to a waveform sampling digitizer (CAEN DT5751) to be digitized and then sent to the DAQ system, as shown in Fig. 2.

The system can be calibrated by using the dark counts of the SiPM without electron irradiation. Figure 3a shows the spectrum distribution of the dark counts. The first peak is the pedestal, and the second peak to the fourth peak correspond to the signals from single photoelectron, two photoelectrons and three photoelectrons, respectively. The calibration factor can be obtained by linear fit of the peaks, as shown in Fig. 3b.

## Test and optimization of the scintillator unit

### Optimization of SiPM coupling configuration

A MIP produces almost the same amount of photons independently on the impact position of the scintillator. When a SiPM is coupled to a scintillator at one position, the light output is depended on the scintillation light propagation distance along the strip to the SiPM coupling point, so the light which is emitted in front of the SiPM window has higher chances to reach the SiPM. This dependence would introduce non-uniformity of the light output, hence affecting the performance of the ECAL. The distribution of the responses to the MIPs over the scintillator strip is characterized by the mean and the spread (RMS). The ratio RMS/mean is defined as non-uniformity of the light output [7]. Figure 4 shows a typical test result of the light output of a BC408 scintillator unit with a Hamamatsu S12571-010P SiPM coupled at one end of the scintillator strip. The non-uniformity of the light output is about 10%.

In order to decrease the non-uniformity of the light output, first the SiPM coupling at different positions of the scintillator strip is tested. A square groove is drilled at
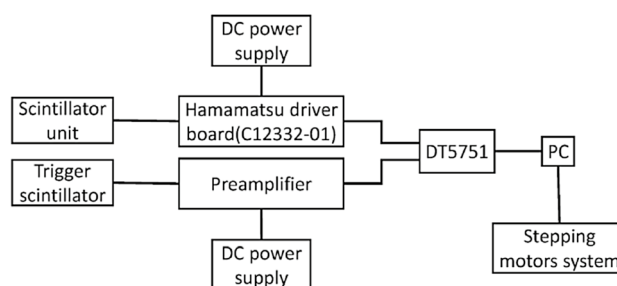


Fig. 1 The schematic of the test system setup



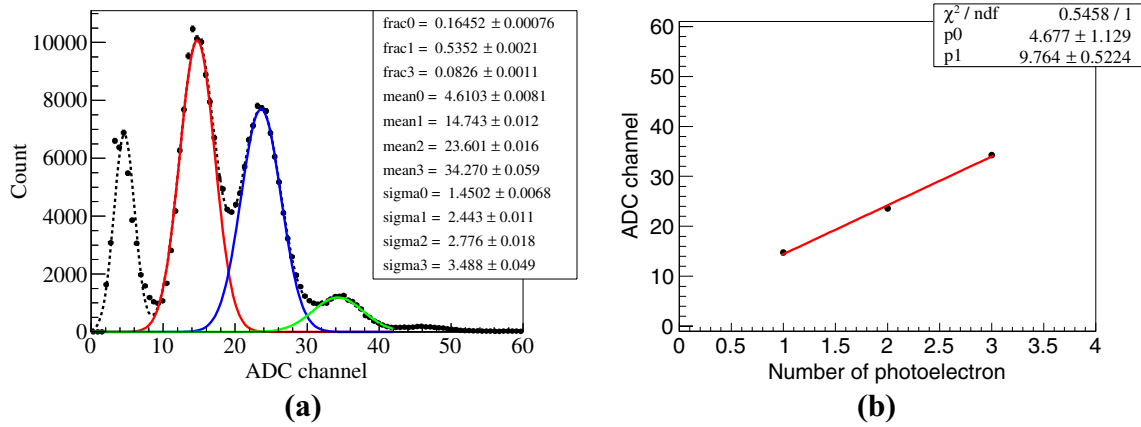Fig. 2 The architecture of the readout electronics

**Fig. 3** Calibration of the test system. **a** The spectrum distribution of the dark counts. **b** Linear fit of the peaks
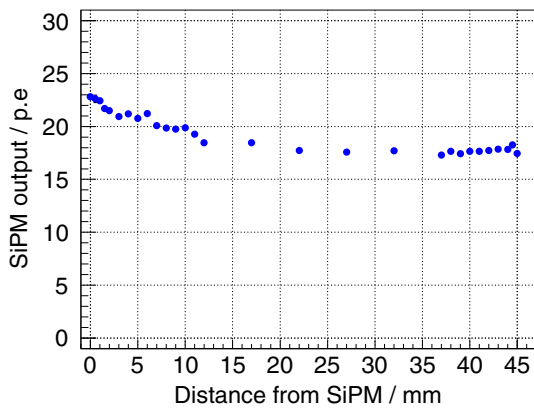


**Fig. 4** Light output and non-uniformity of a scintillator unit with a SiPM coupled at the surface of one end of the strip

the side-end, bottom-center or bottom-end of the scintillator strip to embed the SiPM, as shown in Fig. 5, which are called side-end coupling, bottom-center coupling and bottom-end coupling configuration, respectively. Figure 6 shows the corresponding measured non-uniformities of the scintillator units with different SiPM coupling configurations. The side-end and the bottom-end configurations have

no improvement on the uniformity, while the bottom-center configuration presents a better non-uniformity of about 6%. Furthermore, the bottom-center configuration has additional advantages of completely eliminating dead areas between scintillator strips due to mounting of the SiPMs and allowing to use the SiPMs with large areas which can broaden the dynamic range of the SiPMs.

## Optimization of the groove on the scintillator

Based on the MC simulation, a good uniformity of the light output can be realized by the compensation of the thinner scintillator at the region of the groove for the shorter distance of this region to the SiPM. In order to further improve the uniformity and the light output of the scintillator unit with the bottom-center coupling configuration, the shape and the dimension of the groove are the key parameters that need to be further optimized.

Figure 7 gives the test results of the scintillator units with different groove shapes and dimensions, such as spherical groove, flat spherical groove and runway-shaped groove. The parameters of the grooves are illustrated in Fig. 8; $d$ is the groove depth and $r$ is the radius at the scintillator strip surface. For the scintillator unit with spherical groove
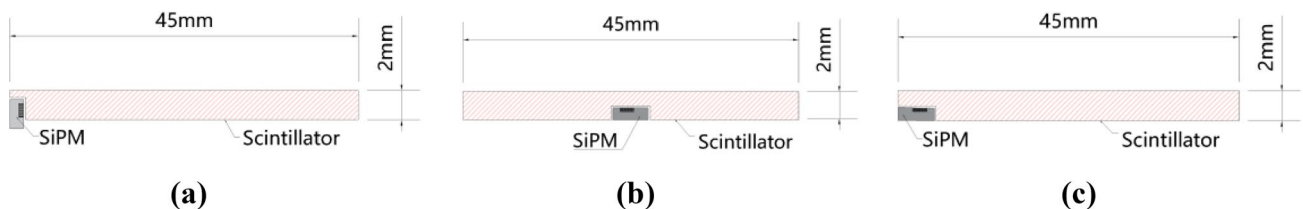


**Fig. 5** Three SiPM-scintillator coupling configurations. **a** A SiPM is embedded into a scintillator strip at one side (side-end). **b** A SiPM is embedded into a scintillator strip at the center of the bottom face (bottom-center). **c** A SiPM is embedded into a scintillator strip at one end of the bottom face (bottom-end)
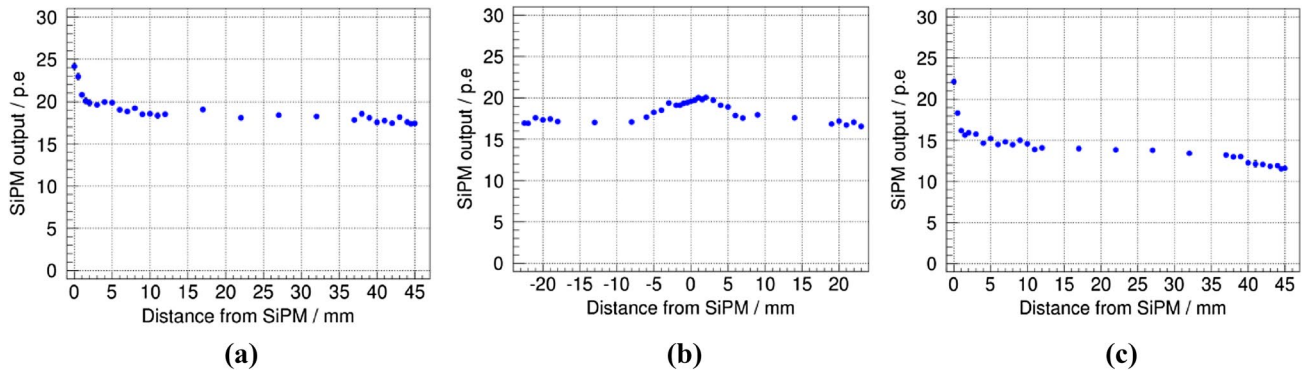
**Fig. 6** Light output of the scintillator units with three different SiPM coupling configurations. **a** Side-end coupling. **b** Bottom-center coupling. **c** Bottom-end coupling
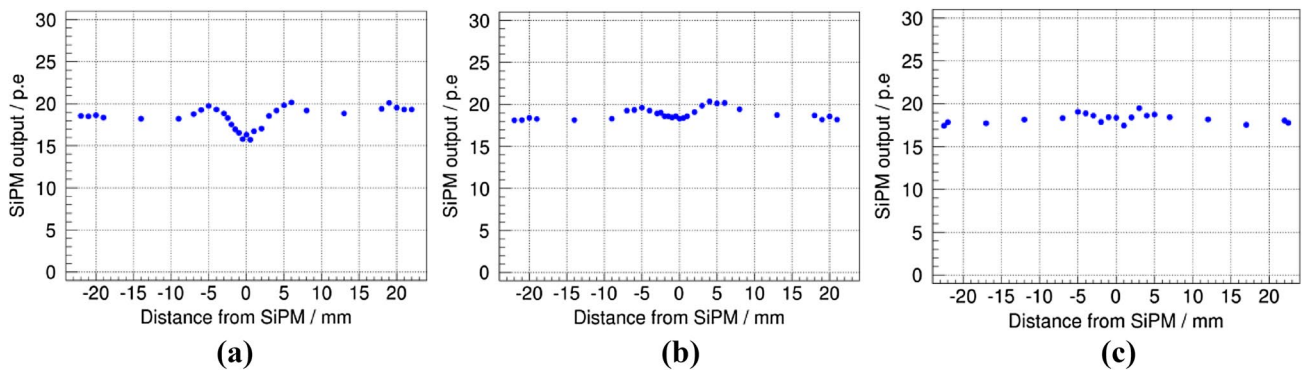


**Fig. 7** Light output of the scintillator strip units with three different groove shapes. **a** Spherical groove. **b** Flat spherical groove. **c** Runway-shaped groove
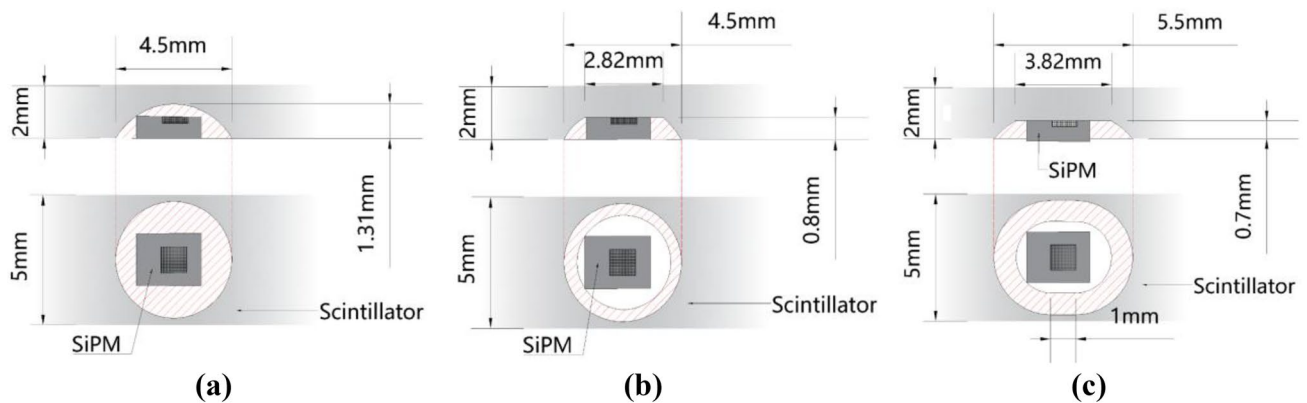


**Fig. 8** The geometry of the grooves. **a** Spherical groove. **b** Flat spherical groove. **c** Runway-shaped groove

(Fig. 8a), the light output at the deepest point is smallest, as shown in Fig. 7a, indicating that the groove depth of about 1.3 mm is overcompensation. So the bottom of the spherical groove is flattened to reduce the groove depth from 1.3 mm to 0.8 mm (Fig. 8b) and increase the light output of this

region. Figure 7b shows the light output of the scintillator unit with the flat spherical groove. As expected, the light output in the deepest region of the groove increases, but the light output in the adjacent regions of the groove is still little larger than the regions far away from the groove.
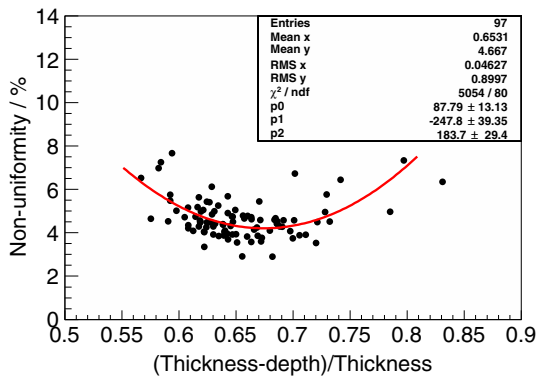
**Fig. 9** Non-uniformities of the light output of the scintillator units change with the relative remaining thickness. The relative remaining thickness is defined as (thickness of scintillator- depth of the groove)/ thickness of scintillator

Based on the test results of the scintillator units with two different grooves mentioned above, the bottom of the spherical groove is first flattened and then extended along a longitudinal length $l$ of the strip to form a runway-shaped groove, as shown in Fig. 8c. The light output of the scintillator units with different parameters of runway-shaped grooves was tested. Figure 9 gives a statistic result of the non-uniformities of the light output changing with the relative remaining thickness of the scintillator. When the relative remaining thickness is about 0.65–0.68, a good uniformity of the light output can be achieved. After the optimization, the optimal parameters of $d = 0.7$ mm, $r = 2.25$ mm and $l = 1.0$ mm were finally determined with respect to the scintillator thickness of 2 mm. The non-uniformity of the light output of the scintillator unit with
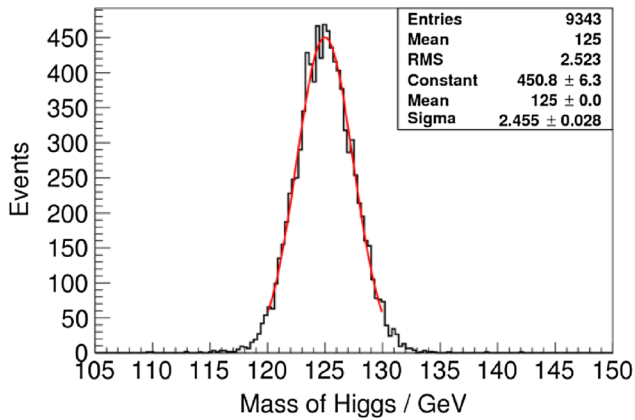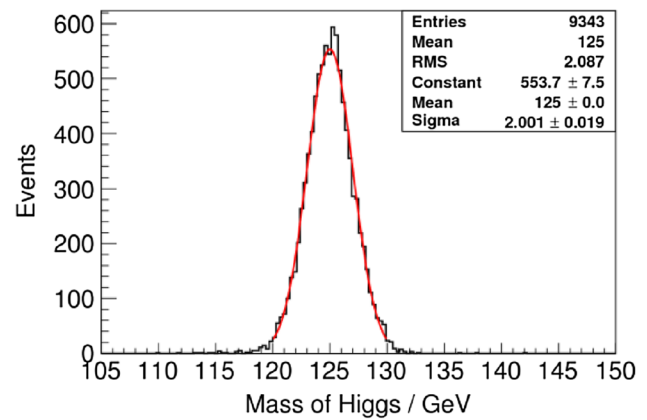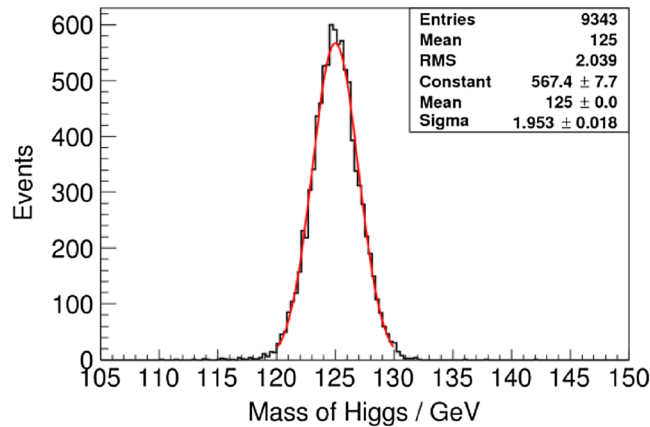


**Fig. 10** Simulation of the construction of Higgs → γγ. **a** The result with the non-uniformity of about 10% (the case of Fig. 4). **b** The result with the non-uniformity of about 4% (the case of Fig. 7c). **c** The result with perfect uniformity
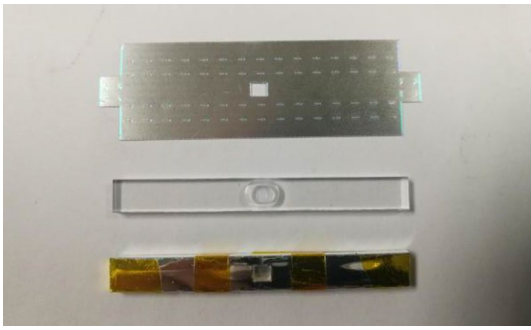
**Fig. 11** Photographs of a piece of ESR film, a scintillator strip and a scintillator strip wrapped with an ESR film

such runway-shaped groove can reach 4% or even better, as shown in Fig. 7c.

## Impact of the non-uniformity on the performance of the ECAL

In order to estimate the impact of the non-uniformity of the light output on the performance of the ECAL, simulation of the construction of Higgs $\rightarrow \gamma\gamma$ was done with different non-uniformities of the scintillator units to get the response. Figure 10a shows the boson mass resolution based on the non-uniformity before optimization (the case of Fig. 4), and Fig. 10b shows the result with the non-uniformity after optimization (the case of Fig. 7c). The boson mass resolution is improved about 23% after the non-uniformity is optimized, which is very close to the case of the scintillator units with perfect uniformity, as shown in Fig. 10c.

## Preliminary test of the scintillator units for a technological prototype

A technological prototype of the ScW ECAL will be constructed and tested with beams, which consists of 30 layers of tungsten absorber plates interleaved with active planes

of about $22.5 \times 22.5$ cm$^2$. Each active plane has about 210 scintillator strip units with a thickness of 2 mm. The thickness of the tungsten absorber layer is 2.8 mm.

In order to study the layout, integration and preliminary performance of the scintillator units before the mass production, about 210 scintillator strips were cut and wrapped with ESR films. Very small holes ($0.01 \times 0.5$ mm$^2$) with 2-mm pitch are made along the crease of the film to make the ESR films can be wrapped tightly on the scintillator strips, as shown in Fig. 11. Moreover, because the light output is sensitive to the reflector close to the SiPM, a hole with almost the same size as the SiPM is opened on the ESR film as the light output window to match the SiPM well. Much bigger hole than the dimension of the SiPM would result in a lower light output and a worse uniformity due to the light leakage. Figure 12 shows the preliminary test results of part of the scintillator units with a runway-shaped groove. The average light output is about 18p.e./MIP, and the average non-uniformity is about 4%. The results verify that the non-uniformity of the scintillator units with the runway-shaped coupling groove at the bottom-center of the strip can be controlled to a low level.

It is worth mentioning that the thickness of the scintillator strip also has an effect on the light output and the uniformity. Usually, the thickness of the scintillator plates from the company has a too big error to be negligible, so the scintillator plates should be thinned on one side to make the thickness uniform before cutting them into strips.

## Conclusion

The scintillator units will play a key role in the CEPC scintillator-tungsten ECAL. In order to get a good uniformity of the light output, the scintillator unit was optimized by the SiPM coupling configuration and the parameters of the coupling groove. The non-uniformity of the scintillator strip with a runway-shaped coupling groove at the bottom-center of the strip can achieve 4% without reduction in the light output. Compared to the original

**Fig. 12** The preliminary test results of the scintillator units with a runway-shaped groove. **a** The light output. **b** The non-uniformity
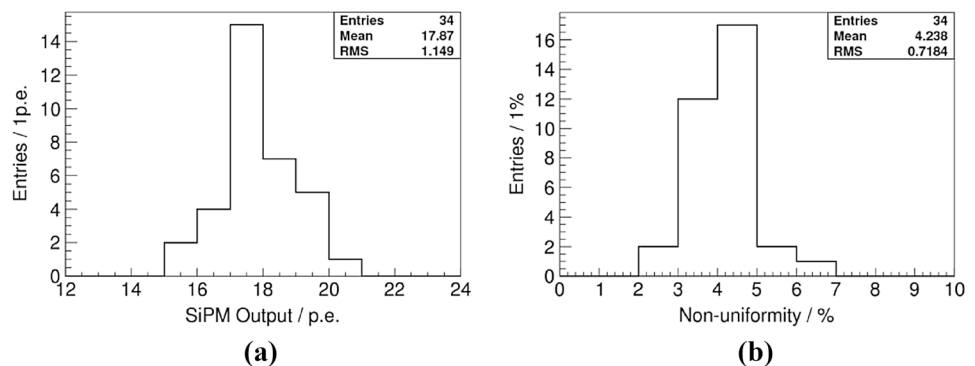
non-uniformity, this optimized uniformity can improve the boson mass resolution of about 23% based on the reconstruction of Higgs → γγ, which is comparable to the perfect homogeneous case. Furthermore, the bottom-center coupling configuration can completely eliminate the dead areas between the scintillator strips due to mounting of the SiPMs and make it possible to use the SiPMs with large sensitive areas which can broaden the dynamic range of the SiPMs. Such coupling configuration can also simplify the operation of the detector construction.

## Compliance with ethical standards

**Conflict of interest** On behalf of all authors, the corresponding author states that there is no conflict of interest.

## References

1. CEPC, CEPC Conceptual Design Report (2018). http://cepc.ihep.ac.cn/CEPC_CDR_Vol2_Physics-Detector.pdf
2. M.A. Thomson, Particle flow calorimetry and the pandora PFA algorithm. Nucl. Instrum. Methods A **611**, 25 (2009). [arXiv: 0907.3577]
3. CALICE collaboration, K. Francis et al., Performance of the first prototype of the CALICE scintillator strip electromagnetic calorimeter. Nucl. Instrum. Methods A **763**, 278 (2014). [arXiv: 1311.3761]
4. CALICE collaboration, J. Repond et al., Construction and response of a highly granular scintillator-based electromagnetic calorimeter. Nucl. Instrum. Methods A **887**, 150 (2018). [arXiv: 1707.07126]
5. CEPC Working Group, H. Yang, Preliminary conceptual design about the CEPC calorimeters. Int. J. Mod. Phys. A **31**, 1644026 (2016)
6. CEPC calorimeter working group, M.Y. Dong, R&D of the CEPC scintillator-tungsten ECAL. JINST **13**, C03024 (2018)
7. B. Bobchenko et al., Optimization of the uniformity of light yield from scintillator tiles readout directly by silicon photomultipliers. Nucl. Instrum. Method A **787**, 166–168 (2015)